II. The Earlies Stages of Stellar Evolution: Protostellar Collapse & Pre-Main-Sequence Contraction

Literature: (Books)
- Stahler & Palla (2004): The Formation of Stars (Whiley VCH)
- Schulz (2006): From Dust to Stars (springer)
- M. D. Smith (2004): The Origin of Stars (World Science Publishers)

Literature: (Reviews)
- MacLow & Klessen (2004), Rev. Mod. Phys. 76, 125
- Bromm & Larson (2004), ARAA, 42, 79
- Larson (2003), Rep. Prog. Phys., 66, 1651
- Shu, Adams, Lizano (1987), ARAA, 25, 23
- McKee & Ostriker (2007), ARAA
- Tohline (1982), Fund. cosm. Phys., 8, 1

- Stars form from gravitationally unstable gas in molecular clouds: prestellar cloud cores
- stars (in particular higher-mass stars) typically form as members of a binary or higher-order multiple system.

- Stars typically form in clusters (of several hundred objects)

II.1. Protostellar Collapse: Jeans mass

- **Gravitational instability:** — **Jeans criterion**

  - often the first approach to determine stability properties is to analyze the linearized set of equations and derive a dispersion relation for the perturbation assumed.
  - Linearized eqn.'s for isothermal self-gravitating fluid:

$$\frac{\partial \rho_1}{\partial t} + \rho_0 \vec{\nabla} \vec{v}_1 = 0 \qquad \text{continuity}$$

$$\frac{\partial \vec{v}_1}{\partial t} = -\vec{\nabla} c_s^2 \frac{\rho_1}{\rho_0} - \vec{\nabla} \phi_1 \qquad \text{momentum}$$

$$\vec{\nabla}^2 \phi_1 = 4\pi G \rho_1 \qquad \text{Poisson}$$

  - ▲ $\vec{\nabla} c_s^2 \frac{\rho_1}{\rho_0} = \frac{1}{\rho_0} \vec{\nabla} p_1$ with $p_1 = c_s^2 \rho_1$ from EOS.
  - ▲ neglecting viscous effects ($\eta = \zeta = 0$)
  - ▲ equilibrium characterized by $\rho_0 = \text{const.}$ and $\vec{v}_0 = 0$
  - ▲ Jeans swindle: Poisson's eqn considers only perturbed potential ($\rightarrow$ set $\phi_0 = 0$)

- with $\frac{\partial}{\partial t}$ [continuity] + $\vec{\nabla}$ [momentum] it follows:

$$\boxed{\frac{\partial^2 \rho_1}{\partial t^2} - c_s^2 \vec{\nabla}^2 \rho_1 - 4\pi G \rho_0 \rho_1 = 0}$$

↳ wave equation for $\rho_1(\vec{x}, t)$

- analyse in Fourier space:

$$\boxed{\rho_1(\vec{x}, t) = \int d^3k \, A(\vec{k}) \, e^{i[\vec{k}\vec{x} - \omega(k)t]}}$$

$\frac{\partial}{\partial t} \mapsto i\omega$. $\quad \vec{\nabla} \mapsto i\vec{k}$.

- dispersion relation:

$$\boxed{\omega^2 = c_0^2 k^2 - 4\pi G \rho_0}$$

▲ if density ρ_0 is small ⟼ disp. rel. of sound waves $\boxed{\omega^2 = c_s^2 k^2}$

▲ or small wavelength $\lambda = \frac{2\pi}{k}$

▲ self-gravity acts "strongest" on <u>large scales</u> (small k)
[gravity is long-range force]

▲ λ increases / k decreases / ρ_0 grows: frequency decreases and eventually $\omega^2 < 0$!

↳ time evolution $\propto \exp(\pm \kappa t)$. (if $\kappa^2 = -\omega^2$)

Exponentially unstable.

- ⟶ Gravitational collapse for wave numbers

$$k^2 < k_J^2 \equiv \frac{4\pi G \rho_0}{c_s^2}$$

- k_J = Jeans wave number
- λ_J = Jeans wavelength = $\frac{2\pi}{k_J} = \left(\frac{\pi c_s^2}{G\rho_0}\right)^{1/2}$
- M_J = Jeans mass = $\frac{4\pi}{3}\rho_0\left(\frac{\lambda_J}{2}\right)^3 = \frac{\pi}{6}\rho_0\left(\frac{\pi c_s^2}{G\rho_0}\right)^{3/2}$

for a spherical perturbation with $\emptyset = \lambda_J$

↳

$$M_J = \frac{\pi^{5/2}}{6}\left(\frac{R}{G}\right)^{3/2} \cdot \rho_0^{-1/2} T^{3/2}$$

$$= \frac{\pi^{5/2}}{6} G^{-3/2} \cdot \rho_0^{-1/2} c_s^3 \qquad c_s^2 = RT$$

- Energy of sound wave $E_{sound} > 0$; $E_{gravitational} < 0$

↳ Instability sets in, when net energy is negative, i.e. when λ exceeds λ_J.

II. 2. Protostellar Collapse: Pressure-free Collapse & Freefall Time scale

- solve hydrodynamic equations in 1D (keep time dependency!)

$$\rho \frac{d\vec{v}}{dt} = -\rho \vec{\nabla}\phi - \vec{\nabla} P \qquad \text{(equ of motion)}$$

$$\frac{d\rho}{dt} + \rho \vec{\nabla}\cdot\vec{v} = 0 \qquad \text{(continuity)}$$

$$\vec{\nabla}\phi = 4\pi G \rho \qquad \text{(Poisson equ.)}$$

- consider special case: no pressure force !!
  - $\frac{d\vec{v}}{dt} = -\vec{\nabla}\phi$
- 1D spherical symmetry: $\vec{\nabla} \rightarrow \frac{d}{dr}$

  $\vec{\nabla}^2 \rightarrow \frac{1}{r^2}\frac{d}{dr}\left(r^2 \frac{d}{dr}\right)$
- Lagrangian description of spherical mass shells: $\frac{dM}{dr} = 4\pi \rho r^2$
  - Poisson: $\frac{1}{r^2}\frac{d}{dr}\left(r^2 \frac{d\phi}{dr}\right) = 4\pi G \rho$

    $\frac{d}{dr}\left(r^2 \frac{d\phi}{dr}\right) = 4\pi G \rho r^2 = G\frac{dM}{dr}$

    (integration)

    $r^2 \frac{d\phi}{dr} = GM$

    $\frac{d\phi}{dr} = \frac{GM}{r^2}$

- in eqn. of motion:

$$\frac{dv}{dt} = -\frac{d\phi}{dr} = -\frac{GM(r)}{r^2} \quad | \cdot 2v\,dt$$

$$2v\,dv = -\frac{GM(r)}{r^2}\,2\cdot v\,dt \quad | \; v = \frac{dr}{dt} \rightarrow v\,dt = \frac{dr}{dt}\,dt = dr$$

$$= -\frac{GM(r)}{r^2}\cdot 2\,dr$$

$$d(v^2) = -2GM\cdot\frac{dr}{r^2} \quad | \text{ integration}$$

$$v^2 = 2GM(r_i)\left(\frac{1}{r} - \frac{1}{r_i}\right) + v_i^2$$

with integration constant v_i^2; assume cloud initially at rest $v_i = 0$ at radius r_i with mass $M(r_i)$

$$\hookrightarrow \quad v(t) = -\left[2GM(r_i)\left(\frac{1}{r(t)} - \frac{1}{r_i}\right)\right]^{1/2}$$

time dependence disguised in $r(t)$

"$-$" because of collapse (radial vector points away from center)

- use $M(r_i) = \frac{4\pi}{3}\rho_i r_i^3$ (cloud is originally homogeneous)

$$\frac{dr}{dt} = -\left[\frac{8\pi}{3}G\rho_i r_i^2\left(\frac{r_i}{r} - 1\right)\right]^{1/2}$$

- substitute $\cos^2\xi = \frac{r(t)}{r_i} \rightarrow \frac{dr}{r_i} = 2\cos\xi\sin\xi\,d\xi$

$$\hookrightarrow \cancel{r_i}\cdot 2\cos\xi\sin\xi\,d\xi = -\left[\frac{8\pi}{3}G\rho_i \cancel{r_i^2}\cdot\left(\frac{1}{\cos^2\xi} - 1\right)\right]^{1/2}\cdot dt$$

$$= +\left[\frac{8\pi}{3}G\rho_i\right]^{1/2}\left[\frac{\sin^2\xi}{\cos^2\xi}\right]^{1/2} dt$$

$$2\cos\xi\,\sin\xi\,d\xi = +\left[\frac{8\pi}{3}G\rho_i\right]^{1/2}\frac{\sin\xi}{\cos\xi}\,dt$$

↳ $$2\cos^2\xi\,d\xi = +\left[\frac{8\pi}{3}G\rho_i\right]^{1/2}dt$$

- use $2\cos^2\xi = 1+\cos 2\xi$:

$$(1+\cos 2\xi)\,d\xi = \left[\frac{8\pi}{3}G\rho_i\right]^{1/2}dt \qquad \text{| integrate}$$

$$\boxed{\xi + \frac{1}{2}\sin 2\xi = \left[\frac{8\pi}{3}G\rho_i\right]^{1/2}\cdot t + C}$$

- with initial condition $r = r_i$ (i.e. $\xi = 0$) at $t = 0$.
  parameter ξ is in general function of <u>both</u> r_i & t !

- freefall time: $r(t) \to 0$: this means $\xi \to \frac{\pi}{2}$
  ↳ this happens in a finite time: τ_{ff}

$$\frac{\pi}{2} + \underbrace{\frac{1}{2}\sin\pi}_{=0} = \left[\frac{8\pi}{3}G\rho\right]^{1/2}\tau_{ff}$$

↳ $$\boxed{\tau_{ff} = \sqrt{\frac{3\pi}{32\,G\rho_i}}}$$ <u>freefall time</u>

- τ_{ff} is a function of initial mean density <u>only</u>.

  for a homogeneous sphere with initial density ρ_i
  <u>all</u> fluid elements have the same τ_{ff}
  ↳ they all arrive at the center at the same time.

- for a homogeneous sphere, the density evolution can be computed analytically:

- use the continuity equ:

$$\frac{d\rho}{dt} + \rho \vec{\nabla}\cdot\vec{v} = 0$$

$$\frac{1}{\rho}\frac{d\rho}{dt} + \frac{1}{r^2}\frac{d}{dr}(r^2 v) = 0$$

$$\frac{d}{dt}(\ln\rho) + \frac{1}{r^2}\frac{d}{dr}(r^2 v) = 0$$

[recall, the divergence in spherical coor. is: $\vec{\nabla}\cdot\vec{A} = \frac{1}{r^2}\frac{\partial}{\partial r}(r^2 A_r) + \frac{1}{r\sin\theta}\frac{\partial}{\partial\theta}(A_\theta \sin\theta) + \frac{1}{r\sin\theta}\frac{\partial}{\partial\phi}(A_\phi)$]

- with $\frac{r}{r_i} = \cos^2\xi$ it follows: $r^2 v = -\frac{\pi}{2\tau_{ff}} r^3 \frac{\sin\xi}{\cos^3\xi}$

and $dt = \frac{4\tau_{ff}}{\pi}\cos^2\xi\, d\xi$

↳ for a general density profile:

$$d\ln\rho = 6\tan\xi\, d\xi\,[1+X]$$

$$\text{with } X = \frac{1}{3}\left[r\frac{d\xi}{dr}(3\tan\xi + \cot\xi) - \frac{d\ln\tau_{ff}}{d\ln r}\right]$$

- for $\rho = \rho_i = \text{const.}$, both τ_{ff} and ξ are independent of radius $\longrightarrow$ $X = 0$ in this case

- integration of $d\ln\rho = 6\tan\xi\, d\xi$ gives

$$\frac{\rho(t)}{\rho_i} = \sec^6\xi$$

if $v_i = 0$

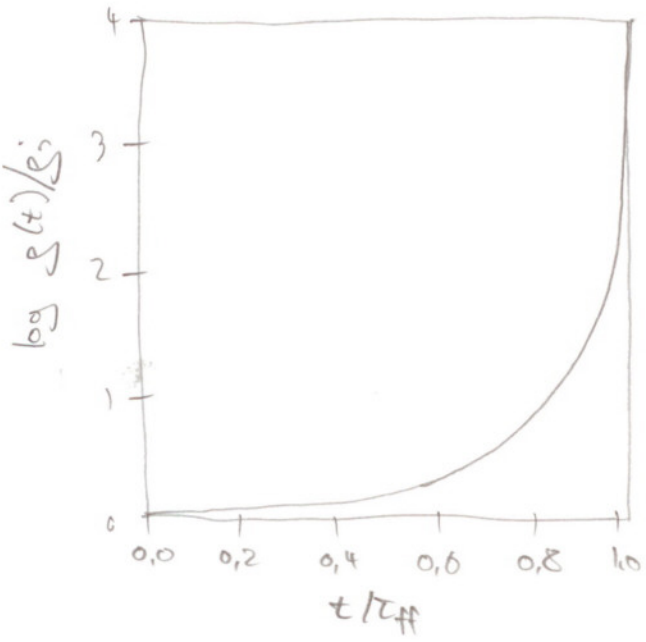

$\frac{\rho}{\rho_i} = 2$ at $t = 0{,}5\ \tau_{ff}$

$\frac{\rho}{\rho_i} = 10$ at $t = 0{,}85\ \tau_{ff}$

- if $\rho_i(r)$ decreases outwards, the central parts have smaller τ_{ff} than outer parts ⟶ inner parts collapse faster ⟶ density profile steepens ⟶ non-homologous nature of gravitational collapse.

(III) gravitational collapse of isolated, isothermal gas spheres

→ similarity sln. a la Shu, Larson, Boston, Hunter, Whitworth, etc...

- hydro eqn's in 1D & spherical symmetry —

closure: $\boxed{P = c_s^2 \rho}$

eqn of motion: $\boxed{\frac{dv}{dt} = \frac{\partial v}{\partial t} + v\frac{\partial v}{\partial r} = -\frac{GM(r)}{r^2} - \frac{c_s^2}{\rho}\frac{\partial \rho}{\partial r}}$ (a) (b)

continuity $\boxed{\frac{dM}{dt} = \frac{\partial M}{\partial t} + v\frac{\partial M}{\partial r} = 0}$ (c)

with $\frac{\partial M(r)}{\partial r} = 4\pi r^2 \rho(r)$

- SIMILARITY SLN. by introducing ONE SINGLE INDEPENDENT VARIABLE $\boxed{\xi = \frac{c_s t}{r}}$ following Hunter (1977)

$\xi = \xi(r,t)$ ξ replaces both r & t !

- set also: $M(r,t) = \frac{c_s^3 t}{G} m(\xi)$

$\rho(r,t) = \frac{c_s^2}{4\pi G r^2} P(\xi)$

$v(r,t) = -c_s U(\xi)$

- THEN (a), (b), (c) reduce to 2 coupled ODE's for P & U and one algebraic eqn. defining $m(\xi)$:

$$\frac{dU}{d\xi} = \frac{(\xi U+1)\{P(\xi U+1) - 2\xi\}}{(\xi U+1)^2 - \xi^2}$$

$$\frac{dP}{d\xi} = \frac{\xi P\{2 - P(\xi U+1)\}}{(\xi U+1)^2 - \xi^2}$$

$$m(\xi) = P\cdot(U + 1/\xi)$$

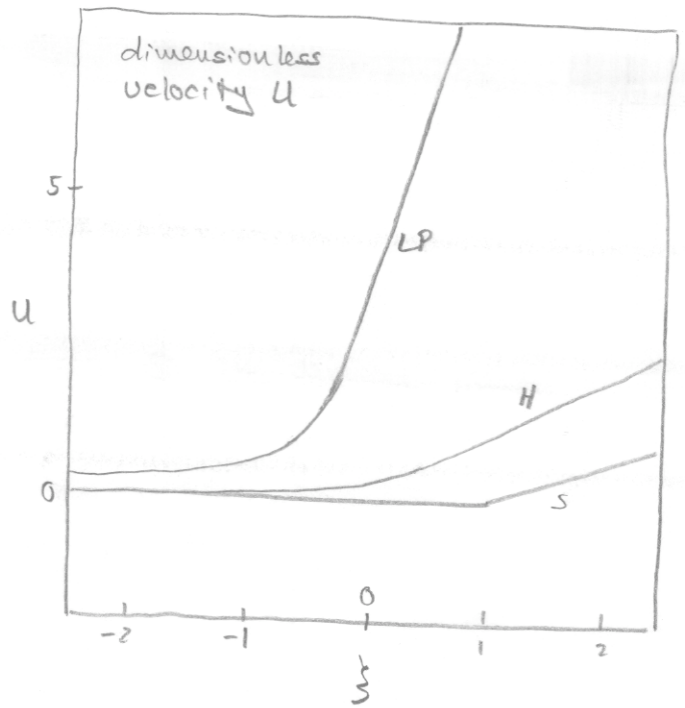

Figures from Hunter (1977)

- He extended the solutions towards $t \to -\infty$ & $t \to +\infty$
- This sln's obey $v \to 0$ for $t \to -\infty$
- $t=0$ is instance of core formation (i.e. occurance of central singularity)
- originally: LP only for $t<0$
  Shu only for $t>0$

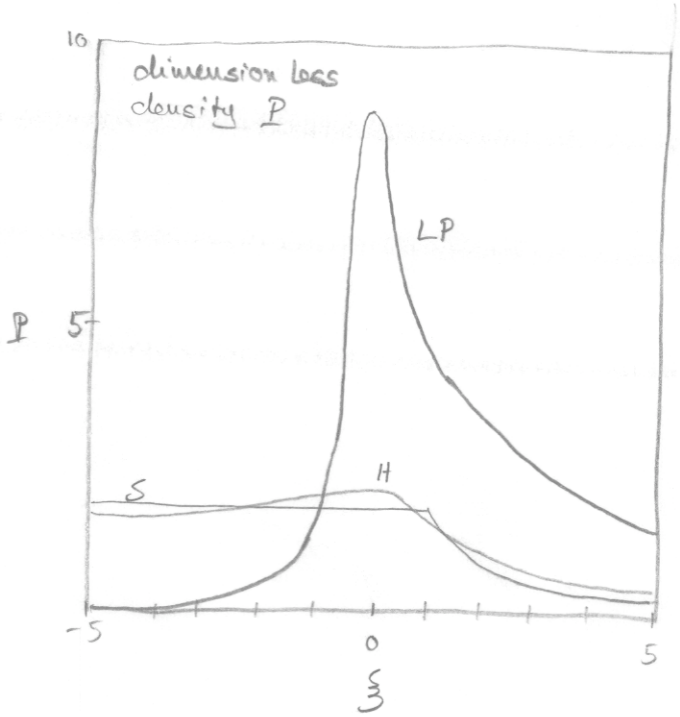

the portion of each curve with zero slope indicates $\rho \propto r^{-2}$

- LP = Larson (1969) - Penston (1969) sln:

at $t \to -\infty$
$\rho = \rho_0 =$ const.
$v = 0$

[collapse of homogeneous sphere from rest]

- S = Shu (1977) sln:

at $t=0$ sis: $\rho = 1/r^2$ & $v=0$

[collapse of singular isothermal sphere]

- H = Hunter (1977) "in between" solution

- Physical insight can be gained by looking at the behavior in various limits:

[A] $\xi \longrightarrow -\infty$

$$U \approx \frac{2}{3}\left(\frac{-1}{\xi}\right) + 45\left[\frac{2}{3} - \exp(Q_0)\right]\left(\frac{-1}{\xi}\right)^3$$

$$\ln\left(\xi^2 I\right) \approx Q_0 + \frac{1}{6}\left[\frac{2}{3} - \exp(Q_0)\right]\left(\frac{-1}{\xi}\right)^2$$

with $Q_0 > 0$. constant

[B] $\xi \approx 0$

$$U \approx U_0 + \xi(I_0 - 2)\xi^2 U_0 + \xi^3\left[(I_0 - 2)\left(1 - \frac{I_0}{6}\right) - \frac{2}{3}U_0^2\right]$$

$$I \approx I_0 - \xi^2\left[\frac{1}{2}I_0(I_0 - 2)\right]$$

with U_0 & I_0 positive constants

[C] $\xi \to +\infty$

$$U \approx \sqrt{2m_0\xi}$$

$$I \approx \sqrt{m_0/2\xi}$$

Numbers	Q_0	U_0	I_0	m_0
LP	0,52	3,28	8,85	46,915
H	11,23	0,295	2,378	2,577
S	$+\infty$	0,0	2,00	0,975

- Conversion into physical quantities (in the various limits)

$\boxed{r \ll c_s \cdot |t| \quad \oplus \quad t<0}$

$$v(r,t) \approx -\frac{2}{3}\frac{r}{-t}$$

$$\rho(r,t) \approx \frac{\exp(Q_0)}{4\pi G} \cdot t^2$$

$\boxed{r \ll c_s \cdot |t| \quad \oplus \quad t>0}$

$$v(r,t) \approx -\left(\frac{2u_0}{c_s}\right)^{1/2} t^{1/2} r^{-1/2}$$

$$\rho(r,t) \approx \frac{1}{4\pi G}\left(\frac{u_0 c_s^3}{2}\right)^{1/2} t^{-1/2} r^{-3/2}$$

$\boxed{r \gg c_s|t| \quad \forall t}$

$$v(r,t) \approx -c_s u_0$$

$$\rho(r,t) \approx \frac{c_s^2 P_0}{4\pi G} r^2$$

- S & LP sln's mutually exclude each other

S: only $0 < \xi < +\infty$; claim is that S describes the accretion flow of an isothermal 1/r2 envelope onto a recently formed protostellar core

LP: only $-\infty < \xi < 0$: transformation of homogeneous sphere into strongly centrally condensed supersonically collapsing cloud.

- $\xi \to -\infty$ $(t \to -\infty)$: initial condition of collapse

$\xi = 0$ $(t=0)$: formation of central zero velocity (and zero radius) core, which for $0 < t \ll -\infty$ grows with $\dot{M} = \frac{c_s^3 u_0}{G}$

$\xi \to +\infty$ $(t \to +\infty)$: very late stages of collapse when most of the original cloud mass is contained in core

Interpretation:

- for any stage of collapse prior to core formation, $t<0$, there will be a region $r \ll c_s(t)$ that is collapsing homologously maintaining uniform density structure and a velocity profile $-v \propto r$.
- there will also be a region $r \gg c_s(t)$ exhibiting constant velocity and $\rho \propto r^{-2}$ density profile
- exactly at $t=0$ the cloud exhibits a $\rho \propto r^{-2}$ profile everywhere (note, the velocity differs for the different models)
- after core formation, $t>0$, there is a region at large radii, $r \gg c_s(t)$, that still has $\rho \propto r^{-2}$ and v a const.,
- while near the center, $r \ll c_s(t)$, the cloud structure will change to $-v \propto r^{-1/2}$ and $\rho \propto r^{-3/2}$.

There are important observable differences between S & LP solution, as discussed in previous lectures.

- Shu accretion rate:

S-slu maintains $\dot{M}(0,t) = \frac{c_s^3 m_0}{G} \quad \forall t > 0$

$$M(0,t) = \underbrace{\frac{c_s^3 t}{G}} \cdot m(\xi)$$

↳ only combination that gives dimension of mass

$[c_s] = \frac{cm}{s}$

$[G] = \frac{cm^3}{g s^2}$

$[t] = s$

- "inside-out" collapse: rarefaction wave moves outward with speed of sound c_s
- at $t=0$ LP & S differ in the velocity field: S → $-v=0$, LP → $-v \gg c_s$

NB: compare Shu rate with Bondi-Hoyle-Lyttleton accretion rate

* Bondi accretion rate: $\boxed{\dot{M}_B = \lambda_c \, 4\pi \rho_\infty \frac{(GM)^2}{c_\infty^3}}$

$\lambda_c = \frac{1}{4} e^{3/2} = 1{,}12$

$\rho_\infty = \rho$ at ∞

$c_\infty = c_s$ at ∞

* Shu rate: $\boxed{\dot{M}_s = \frac{c_s^3}{G} \cdot m_0}$

$m_0 = 0{,}975$

* if we set $c_s = c_\infty$, and if we set $M = \dot{M} \cdot t$, and if we identify $4\pi G \rho_\infty = t^{-2}$ with the inverse square of the free-fall time, then we see:

$$\dot{M}_B = \lambda_c \frac{1}{t^2 G} \frac{G^2}{c_\infty^3} \cdot \dot{M}_B^2 t^2$$

$$1 = \lambda_c \frac{G}{c_\infty^3} \cdot \dot{M}_B$$

$$\dot{M}_B = \frac{1}{\lambda_c} \frac{c_s^3}{G} \approx \dot{M}_s \quad \text{as } \lambda_c^{-1} \approx m_0 \qquad \checkmark$$

* Bondi problem: spherical accretion of gas by a gravitating point mass M. (self-gravity of gas is ignored.)

* Hoyle-Lyttleton: if * moves with v_* through the medium

$$\dot{M} = \lambda_* \, 4\pi \rho_\infty \frac{(GM)^2}{(v_*^2 + c_\infty^2)^{3/2}}$$

* in REALITY: NO SIS ⟹ time varying $\dot{M}$

Example 1 multiple power law:

compare, e.g., with density profile of B68 or the sample of prestellar cores by Bacmann et al. (2000)

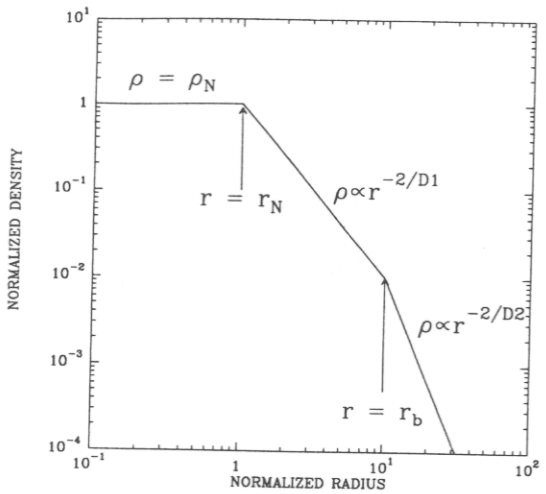

Fig. 3. Density *vs.* radius (in log–log format) for an idealized pre-stellar cloud with a flat nucleus surrounded by a power-law envelope and a steeper power-law outer boundary

resulting accretion rates

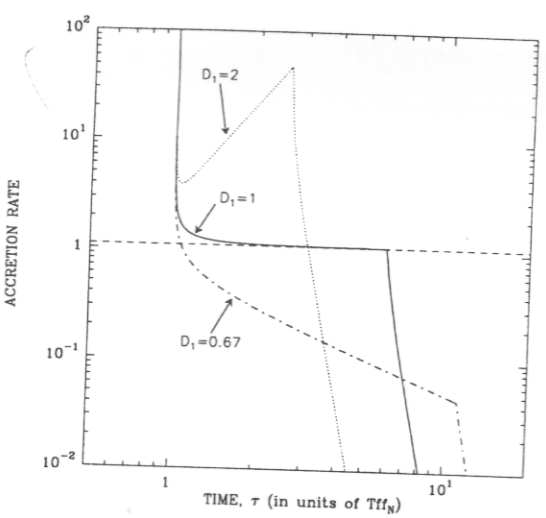

Fig. 5. Accretion rate as a function of time for three values of D_1 corresponding to r^{-1} (dotted curve), r^{-2} (solid curve), and r^{-3} (dash-dotted curve) envelopes respectively in the initial density profile. A sharp outer edge ($\bar{r}_b = 10$ and $D_2 = 0.1$) has been assumed in all three cases. The dashed horizontal line gives the asymptotic value of the accretion rate obtained in the case an r^{-2} initial density profile

(from Henriksen et al. 1997)

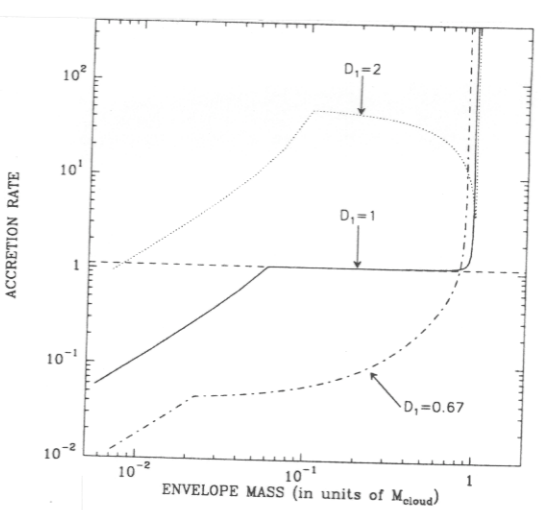

Fig. 6. Absolute value of the accretion rate as a function of envelope mass for the same three initial density profiles as in Fig. 4 and Fig. 5. Here again, the dashed horizontal line gives the asymptotic value of the accretion rate predicted in the case an r^{-2} initial density profile

example 2: Plummer sphere (modeled to fit L1544)

generalized Plummer density distribution

$$\rho(r, t=0) = \rho_{core} \cdot \left[\frac{r_{core}}{(r_{core}^2 + r^2)^{1/2}} \right]^{\eta}$$

original Plummer sphere: $\eta = 5$

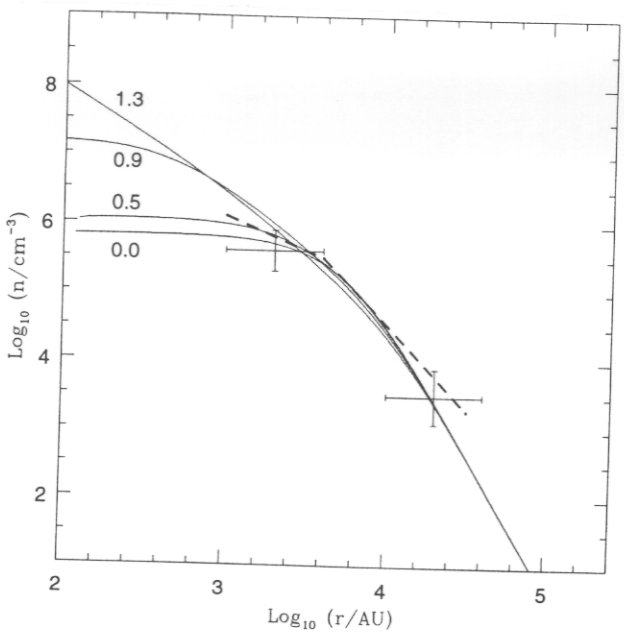

FIG. 1.—Volume-density profiles. Each curve is marked with the value of t/t_0, where the central point-mass forms at $t = t_0$, so $t/t_0 < 1$ corresponds to contracting prestellar cores, and $t/t_0 > 1$ corresponds to young class 0 protostars. The dashed line shows the density profile of L1544 derived from IRAM 1.3 mm continuum mapping by Ward-Thompson et al. 1999. The crosses are the volume-density and radius values inferred by Tafalla et al. 1998 and Williams et al. 1999 for L1544. Hence, all of these observations of L1544 are consistent with $t/t_0 \sim 0.5$.

(from Whitworth & Ward-Thompson 2001)

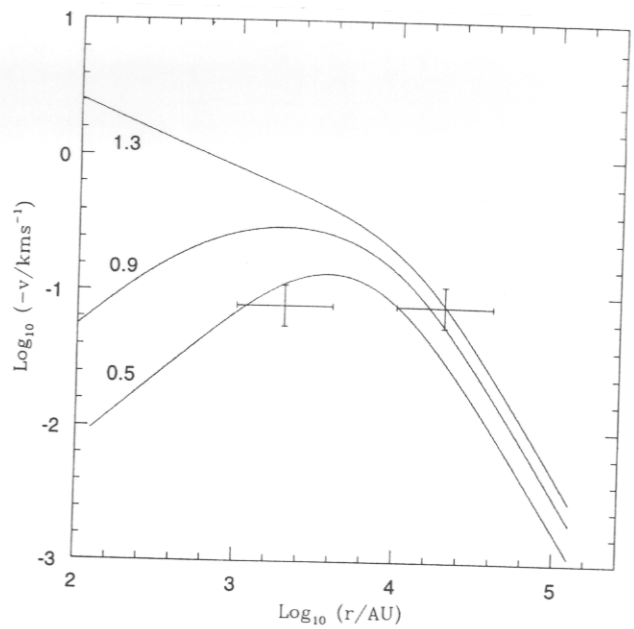

FIG. 2.—Inward radial velocity profiles. Each curve is marked with the value of t/t_0, as in Fig. 1. The crosses represent the infall velocities inferred by Tafalla et al. 1998 and Williams et al. 1999 for L1544. Once again, a value of $t/t_0 \sim 0.5$ is consistent with the observations.

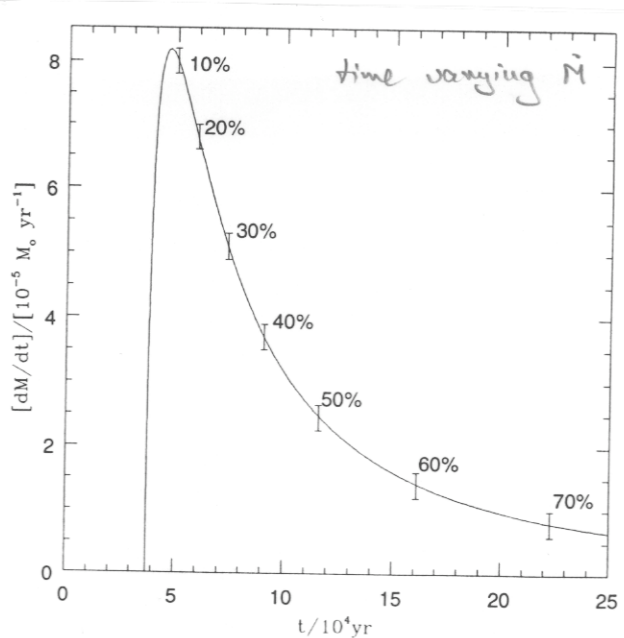

FIG. 3.—Accretion rate, in units of $10^{-5} M_\odot$ yr^{-1}, plotted against time, in units of 10^4 yr. The borderline between prestellar cores and class 0 protostars occurs when the accretion rate first becomes non-negligible. The tick marks indicate the fraction of the total mass that has reached the central protostar. The class 0/I borderline occurs when this fraction is 50%.

⑤ Models of 1D collapse

* Effects of EOS:

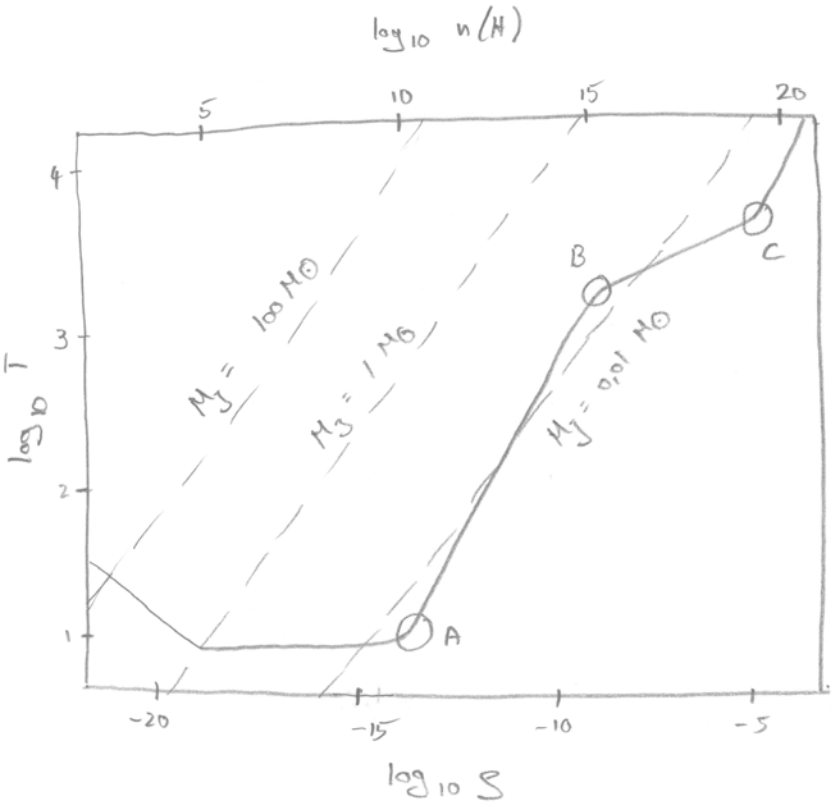

(from Bodenheimer 1980)

S-T condition in the center of a $3M_\odot$ protostar

(A) end of isothermal phase

(B) onset of H_2 dissociation

(C) end of H_2 dissociation, begin of final adiabatic core

1) At low densities, 10^{-19} g cm^{-3} $\lesssim \rho \lesssim 10^{-13}$ g cm^{-3}, the molecular cloud collapses isothermally ($\gamma \approx 1$) because the gas is optically thin to its primary cooling radiation (infrared radiation from dust grains) and the compressional heat generated by collapse can be readily radiated away.

2) At densities above $\sim 10^{-13}$ g cm^{-3} (point A in the figure), the cloud is opaque to this radiation, so the gas heats up, following an adiabat $\gamma \approx 7/5$ that is appropriate for its primary constituent, molecular hydrogen (see DeCampli *et al.*, 1978). The exact density at which adiabatic collapse sets in is governed by how much material surrounds and obscures the center of the cloud. As shown, for a 3 $M_\odot$ cloud it occurs at $\rho \sim 10^{-14}$ g cm^{-3}; for a 1 $M_\odot$ cloud it is closer to 10^{-13} g cm^{-3}; for a cloud more massive than 3 $M_\odot$, complete obscuration sets in at $\rho < 10^{-14}$ g cm^{-3}.

3) At a temperature ~ 2000 K (point B in the figure), molecular hydrogen dissociates by an endothermic reaction, so over the range of densities 10^{-8} g cm^{-3} $\lesssim \rho \lesssim 10^{-4.5}$ g cm^{-3}, much of the compressional heat of collapse is used up dissociating H_2. The resulting adiabatic exponent in this range of densities is $\gamma \approx 1.1$.

4) Once H_2 has been completely dissociated (point C in the figure), further compression of the essentially monatomic gas causes the central temperature to rise along a $\gamma \approx 5/3$ adiabat.

(from Tohline 1982)

* physical processes during 1D collapse
(from Tohline 1982, Fund. Cosm. Phys.)

Beginning with Larson (1969), many detailed numerical models have followed the spherical hydrodynamic collapse of a 1 $M_\odot$ gas cloud along a variable adiabat similar to the one shown in Figure 10. These models will not be discussed individually here; they have been adequately summarized by Winkler and Newman (1980a, b) and in the introduction to a series of papers on this collapse problem by Stahler, Shu and Taam (1980a).

The spherical collapse of a molecular cloud having a mass $M \sim 1\ M_\odot$ can be divided into two parts: the *hydrodynamic collapse phase* itself, which begins from a Jeans unstable, low density gas cloud and ends with the formation of a small, hydrostatic core at densities $\sim 10^{-4}$–10^{-2} g cm^{-3}; and the accretion phase during which a free-falling envelope, perhaps containing a substantial fraction of the cloud mass, accretes through a shock front onto the hydrostatic core. As alluded to in §5, the accretion phase is difficult to model accurately. An accurate treatment demands an implicit hydrodynamic scheme with spatial resolution sufficient to resolve the strong accretion shock that separates the hydrostatic core from the free-falling envelope. Winkler and Newman (1980a, b) have provided a definitive analysis of the spherical collapse problem from a configuration initially near the Jeans limit through the entire accretion phase. The accretion phase by itself has been studied in detail by Stahler, Shu, and Taam (1980a, b, 1981) using a unique mathematical approach to the problem. Basically, these groups have shown that although Larson's (1969) original models of spherical collapse encompassed some major simplifying assumptions, his models predict fairly accurately the observable properties of a protostar during its final accretion phase. The work of these two groups should be consulted for a complete discussion of this important phase of protostellar collapse.

The variable adiabat of Figure 10 introduces some interesting features into the hydrodynamic collapse phase of a protostellar cloud's evolution. In order to aid in the physical interpretation of these features, lines of constant Jeans mass have been plotted in the figure for $M_J = 100\ M_\odot$, 1 $M_\odot$, and 0.01 $M_\odot$, assuming a mean molecular weight $\mu = 2$ in each case. If, for example, a 1 $M_\odot$ molecular cloud lies somewhere on the solid ρ–T curve to the left of the $M_J = 1\ M_\odot$ dashed line, that cloud will be prevented from collapsing because $M < M_J$, or equivalently $\alpha < 1$ for the cloud. If the cloud's properties put it somewhere to the right of the $M_J = 1\ M_\odot$ line, $\alpha < 1$ for the cloud and it will collapse along its appropriate ρ–T curve.

A 1 $M_\odot$ cloud that is barely Jeans unstable begins its evolution at a density $\rho_I \sim 10^{-18}$–10^{-19} g cm^{-3} near the intersection of the solid ρ–T curve and the dashed $M_J = 1\ M_\odot$ line in Figure 10. As its density increases, it remains isothermal at about 10 K until it becomes opaque to its cooling radiation near point A on the ρ–T curve. Many investigators, beginning with Penston (1966) and Bodenheimer and Sweigart (1968), have found that during this isothermal phase of collapse the cloud develops a strongly centrally condensed structure ($\rho \propto r^{-2}$) independent of its initial density structure. At point A the centralmost, highest density region of the cloud is the first volume of material to become opaque. A hydrostatic core, possessing only a small fraction of the total cloud mass, forms. This core then accretes the infalling envelope material through a shock front. As the core increases in mass, its temperature rises following the $\gamma \sim 7/5$ adiabatic part of the solid ρ–T curve in Figure 10. At the point (B) of H_2 dissociation, the central part of this core becomes unstable toward a second collapse. This second collapse stops when dissociation is complete (point C in the figure) and a second (inner) hydrostatic core forms. Accretion of envelope material through a second shock onto this inner core allows the core to grow in mass and causes the central cloud temperature to increase along the $\gamma \sim 5/3$ adiabatic part of the ρ–T curve in Figure 10. The formation of this second core begins what has been termed above the accretion phase of the collapse.

The reason a double core structure develops during this collapse can be understood in relatively simple physical terms. At point A in Figure 10 the Jeans mass is $M_J \sim 0.004\ M_\odot$ (assuming $\mu = 2$). Therefore, from Eq. (6.1), if the entire one solar mass of gas reached this point in the ρ–T diagram at exactly the same time, the value of α for the cloud would be $\alpha \sim 0.025$, and the cloud would be far from virial equilibrium. However, in the collapse just described, the cloud is very centrally condensed by the time it evolves to point A so much less than 1 $M_\odot$ of the gas hits point A initially. The centralmost volume enclosing $\sim 0.004\ M_\odot$ is actually able to approach virial balance at point A because (1) $\alpha \sim 1$ for that small volume of gas, (2) the adiabatic exponent for further compression of that volume is greater than 4/3, and (3) its own dynamic readjustment time scale is short compared to the collapse time of the rest of the lower density cloud. Accretion of material onto this

small mass core increases its mass and pushes it up the $\gamma \sim 7/5$ adiabat to point B in Figure 10. At point B, $M_J \sim 0.017\ M_\odot$ (assuming $\mu = 2$), so when more than $\sim 0.017\ M_\odot$ of gas has entered the core, α drops below unity and γ becomes less than 4/3, so the core itself becomes Jeans unstable toward further dynamic collapse. Because the core is centrally condensed, its centralmost volume leads the collapse to point C where again virial balance is attainable by a fraction of the mass. $M_J \sim 0.002\ M_\odot$ (assuming $\mu = 1$) at point C, so for the same reasons that the first core formed, a second (inner) core can form when $\sim 0.002\ M_\odot$ hits the ρ–T conditions of point C. Accretion then pushes this inner core up the $\gamma \sim 5/3$ adiabat to ρ–T conditions that allow a larger and larger mass core to maintain virial balance. This simple "virial balance" explanation for why the double core structure forms gives a surprisingly accurate prediction of what the value of the mass in the first and second cores should be when they first form. Larson (1969) found in his calculations that the first core initially had a mass $\sim 0.005\ M_\odot$ and the second core had a mass $\sim 0.0015\ M_\odot$.

The formation of the double core structure clearly hinges on the fact that the cloud collapses in an extremely nonhomologous fashion. Its centrally condensed, nonhomologous structure developed, in turn, because the isothermal collapse began from a configuration near the Jeans limit. The double core structure can probably be bypassed by any cloud that (1) collapses from an initial configuration that is very Jeans unstable ($\alpha \ll 1$) and (2) is not extremely centrally condensed initially. The negligible effects of pressure in such a model will prevent the centrally condensed, isothermal similarity flow from developing and the comparatively homologous nature of the pressure-free collapse will allow a substantial part of the cloud's central volume to reach point A at essentially a single instant in time. If this central volume encloses a mass $\geqq 0.017\ M_\odot$, it will be unable to attain virial balance at any temperature below that required to dissociate H_2 and force the cloud to bypass the formation of a low density, first core. Narita, Nakano and Hayashi (1970) have presented results from the collapse of an initially very Jeans unstable $1\ M_\odot$ gas cloud where the formation of a low density hydrostatic core did not occur. This result is not surprising in light of the physical arguments just given.

The formation of the double core structure in itself is not particularly significant in a spherical collapse calculation. Bodenheimer (1972, p. 34) has pointed out that the central conditions at the time of the formation of the final "stellar" core are practically independent of initial conditions and specifically do not depend on the presence of a first hydrostatic core. The double core structure has been emphasized here, however, because as we shall see its role may be significant in multidimensional evolutions.

The accretion phase of an evolution can have substantially different observable properties depending on whether $\alpha_i \sim 1$ or $\alpha_i \ll 1$ in a cloud. A very Jeans unstable model, such as the one evolved by Nakano, Narita and Hayashi (1970), will possess a much more luminous and much shorter accretion phase than will a model that is only barely Jeans unstable initially, such as the one evolved by Larson (1969) and by Winkler and Newman (1980a, b). The accretion luminosity L_{acc} is different basically because it is proportional to the rate dm/dt at which the cloud's envelope mass accretes onto the hydrostatic core (Winkler and Newman, 1980a). This rate in turn is (Stahler, Shu and Taam, 1980a)

$$\frac{dm}{dt} \sim M\ \tau_{ff}^{-1} \tag{6.3}$$

where M is the cloud mass. Since $\tau_{ff}^{-1} \propto \rho_i^{1/2}$, it is clear that an initially high density cloud ($\alpha_i \ll 1$) will collapse faster and have a larger accretion luminosity than an initially low density cloud ($\alpha_i \sim 1$).

Since an important observable property of the protostellar collapse does depend on the conditions in the cloud at the onset of collapse, it would be nice to have some idea of which model, $\alpha_i \ll 1$ or $\alpha_i \sim 1$, is more likely to arise in the interstellar medium. An answer to this is not yet available. In light of the conclusions of §§3 and 4, it should be emphasized that only the $\alpha_i \sim 1$ model stands a chance of undergoing a reasonably spherical collapse. Being essentially pressure-free initially, any $\alpha_i \ll 1$ model would be susceptible to flattening and would have a tendency toward fragmentation. The results of spherically symmetric collapse calculations seem physically appropriate only for gas clouds that begin their collapse from configurations near the Jeans limit.

(6) Collapse in 3D ⟶ binary formation

* almost ALL stars form as part of a binary or higher-order multiple system
* prestellar cores have angular momentum ($j \approx 10^{20} - 10^{22}$ $\frac{cm^2}{s}$)
* ⟹ formation of rotationally supported disk during collapse
* further protostellar mass accretion via viscous transport processes (see next lectures)
* often disk "too massive" ⟶ grav. instability ⟶ binary formation by disk fragmentation
* for a recent review see Bodenheimer et al (2000, PP IV)

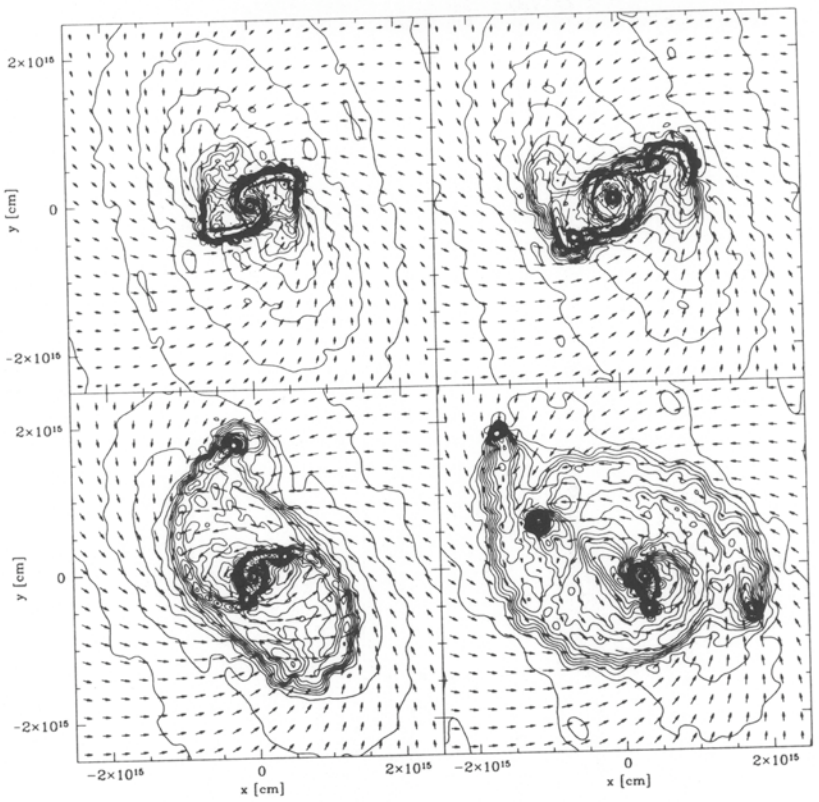

Figure 3(b). The evolution of the same cloud that is shown in part (a), calculated with an SPH code. Symbols and curves have the same meaning as in part (a). (upper left) $t = 1.135 \times 10^{12}$ s; $\log \rho_{max} = -10.0$; $\Delta \log \rho = 0.25$; $V_{max} = 2.44 \times 10^5$ cm s^{-1}. (upper right) $t = 1.160 \times 10^{12}$ s; $\log \rho_{max} = -9.7$; $\Delta \log \rho = 0.25$; $V_{max} = 2.88 \times 10^5$ cm s^{-1}. (lower left) $t = 1.175 \times 10^{12}$ s; $\log \rho_{max} = -9.6$; $\Delta \log \rho = 0.25$; $V_{max} = 3.66 \times 10^5$ cm s^{-1}. (lower right) $t = 1.190 \times 10^{12}$ s; $\log \rho_{max} = -9.5$; $\Delta \log \rho = 0.25$; $V_{max} = 3.38 \times 10^5$ cm s^{-1}. From Burkert et al. (1997).